Available online at www.sciencedirect.com

ScienceDirect

Catalysis Today 118 (2006) 392–401

CATALYSIS TODAY

www.elsevier.com/locate/cattod

Methane oxidation – effect of support, precursor and pretreatment conditions – in situ reaction XPS and DRIFT

Martin Schmal[a,*], Mariana M.V.M. Souza[b,1], Violeta Virginia Alegre[b,1],
Mônica Antunes Pereira da Silva[b,1], Deborah Vargas César[a],
Carlos A.C. Perez[a]

[a] NUCAT/PEQ/COPPE, Federal University of Rio de Janeiro, Centro de Tecnologia, Bloco G,
sala 128, Cidade Universitária, CEP: 21945-970, Rio de Janeiro, RJ, Brazil
[b] Escola de Química, Federal University of Rio de Janeiro, Centro de Tecnologia, Bloco E,
Cidade Universitária, CEP: 21949-900, Rio de Janeiro, RJ, Brazil

Abstract

The methane combustion was studied on Pd supported catalysts searching for explanation of the effects of support, pretreatment and induction periods on the activity of the Pd/alumina, Pd/zirconia, Pd/niobia and Pd/niobia/alumina catalysts. Characterization of methane oxidation in XPS and DRIFTS chambers indicated that an induction period of at least 6 h is necessary to form Pd in a higher oxidation state $Pd^{2+\delta}$ coexisting with PdO as the surface active phases. Similarly, DRIFTS measurements showed distinct species at the surface during the oxidation of methane after 6 h, indicating formate species on Pd/Alumina and CH_x-species and O_2^- adsorption on the Pd/zirconia catalyst, suggesting different reaction mechanisms. The reverse pathway depends on the surface modification due to the temperature and induction time.

The activity of the Pd/niobia/alumina was better than of the Pd/niobia. The effect of the precursor was observed, indicating that palladium nitrate precursor allows to lower dispersion but better performance on methane oxidation. The stability was studied and shows that the Pd/zirconia catalyst was stable and is regenerated, while the Pd/alumina catalyst deactivates very fast and is not regenerated. The effect of pretreatment of the catalysts on the methane oxidation showed different behavior depending of the support.

Keywords: Methane; Combustion; Palladium; Alumina; Zirconia; Niobia

1. Introduction

Catalytic combustion on stabilized catalysts is one of the most attractive alternatives for elimination of gases and has been studied intensively in the last 10 years. Antipollutants catalysts based on palladium are the most active for methane combustion being largely studied employing alumina, silica and other modified supports.

Pd-based catalysts are very active for complete oxidation of methane [1] and depending on the support the PdO clusters require temperatures above 600 K and in general high Pd concentrations, inhibiting oxidation of methane at low temperatures [2–4].

Garbowski et al. [5] proposed a redox mechanism for the total methane oxidation: first, a strong adsorption of O_2 on metallic particles producing superficial palladium oxide; followed by adsorption and reaction of methane on these oxide sites with restoration of reduced sites of palladium. Consequently, palladium surface could change constantly from an oxide to a reduced state and vice-versa.

However, there are still some controversies related to catalyst performance regarding the active phase, the amount of Pd, metallic precursor, pre-treatment and reaction conditions [1–3,6]. Two controversies remain regarding whether the reaction is or not structure sensitive [7] and if the oxidation state of palladium is Pd^0, PdO or a mixture of both [3,7]. Due to the high exothermic effect during methane oxidation, the structure and oxidation state of palladium can be modified during the reaction.

Many oxides as La_2O_3, TiO_2 and Nb_2O_5 have been studied as promoters for catalysts based on noble metals for use in

---

* Corresponding author. Tel.: +55 21 2562 8352; fax: +55 21 2562 8300.
E-mail address: schmal@peq.coppe.ufrj.br (M. Schmal).

[1] Fax: +55 21 2562 7631.

0920-5861/$ – see front matter © 2006 Elsevier B.V. All rights reserved.
doi:10.1016/j.cattod.2006.07.026

hydrocarbon oxidation. These oxides dispersed over alumina modify the metallic phase on different aspects such as degree of reducibility, metal–support interaction, dilution of active phases, among others [8–10].

Fujimoto et al. [11] studied the activation during the induction period and explained this behavior through the oxygen-deficient PdO_x crystallites on zirconia support, which were found intentionally or accidentally during decomposition of impregnated Pd precursor salts.

Eppling and Hoflund [12], one year later, found out through XPS measurements that near the surface region the entered catalyst consists mostly of PdO and ZrO_2 with some Pd metal. The presence of metal sites allows the dissociative adsorption of CH_4 to compete with O_2 adsorption and since oxidation of methane does not occur over supported Pd metal, dissociated methane fragments spilt onto the support surface to Pd-oxide region and then oxidizes. Recently, Li et al. [13] studied this reaction using in situ FTIR experiments and showed the formation of intermediate species, which are responsible for the reaction.

Thevenin et al. [14] studied cerium-doped palladium catalysts with La and Ba and concluded that Ce enhanced the thermal stability of alumina but not the activity and, on the contrary, the activity decreased. However, with La and Ba doped materials the presence of Ce increased their activity. Through XPS measurements these doped catalysts enhanced the reduction of PdO into Pd, and more than 60% of them were reduced on the PdLaCe catalyst. The Pd/PdO ratios were also determined. However, the conversion with increasing temperature reached a maximum around 700 K and then decreased, which was attributed to the transition between the active species PdO and Pd^0.

The main objectives of this work are to study what occurs differently for the methane combustion during the induction period on the Pd/Al_2O_3 and Pd/ZrO_2 catalysts and how XPS and DRIFTS do explain the differences of the nature of Pd species under reaction conditions. It also investigates the effect of the support, in particular the niobia-modified alumina supported palladium catalyst and the effect of the precursor on the methane combustion when compared to Pd/Al_2O_3 catalyst.

2. Experimental

2.1. Preparation and characterization of catalysts

A commercial γ-Al_2O_3 from Harshaw (BET area: 200 m^2/g) and ZrO_2 (BET area: 62 m^2/g), obtained by calcination of zirconium nitrate (Aldrich) in air at 550 °C for 2 h, were used as supports. Pd was added from a $PdCl_2$ (Aldrich) precursor by incipient wetness impregnation of the supports. The precursor was dissolved in concentrated HCl to generate tetrachloride palladium acid (H_2PdCl_4), heated to eliminate chlorine, dissolved in distilled water, dried and again diluted until the final volume. The samples were dried overnight in an oven and then calcined in air at 550 °C for 2 h. Palladium contents were close to 1 wt.%.

Niobia-modified alumina support with 10% of Nb_2O_5 was prepared by the impregnation method of γ-Al_2O_3 (Pural SB of Condea, 178 m^2/g) from aqueous solution of ammoniacal complex of niobium (CBMM) for 16 h. Sample was then dried at 80 °C for 16 h and calcined under air flow at 550 °C (2 °C/min), during 16 h. Palladium was introduced by dry impregnation with an aqueous solution of $Pd(NO_3)_2$. Sample was re-calcined under air flow at 500 °C during 2 h. The same methodology was used to prepare catalyst with 1 wt.% Pd supported over alumina and niobia. The samples were denoted as PdAl, PdNb for the oxide supports alumina and niobia, respectively, and Pd10NbAl.

The composition of the catalysts was analyzed by X-ray fluorescence (XRF) using a Rigaku Rix 3100 spectrometer. N_2 adsorption and desorption measurements were carried out at −196 °C in an ASAP 2000 Micromeritics automatic device. The sample (200 mg) was previously treated at 300 °C for 3 h under vacuum of 10^{-1} Torr.

CO chemisorption analyses was obtained at room temperature using an automatic adsorption system (ASAP 2000, Micromeritics). The samples were pretreated with He flux at 150 °C for 1 h. After reduction at 500 °C under 10%H_2/Ar flow, the samples were evacuated at 10^{-6} Torr for 30 min at the reduction temperature and cooled to room temperature. Irreversible CO uptakes were obtained from the total and reversible adsorptions isotherms taken in a pressure range of 50–400 mmHg.

2.2. Catalytic tests

The reactions were carried out in a fixed-bed flow-type quartz reactor loaded with 20 mg of catalyst, under atmospheric pressure. The catalysts were dried in situ with flowing nitrogen at 150 °C before reduction with 10%H_2/N_2 (30 mL/min) for 1 h at 500 °C. After reduction the catalyst was purged with nitrogen for 30 min at the same temperature. The total feed flow rate was held constant at 200 cm^3/min, with ratio of CH_4:O_2:He = 1:2:17 or 1:4:15. The activity tests were performed at different temperatures, ranging from 250 to 700 °C, in steps of 50 °C that were kept for 30 min at each temperature. The reaction products were analyzed by on-line gas chromatograph (CHROMPACK CP9001), equipped with a Hayesep D column and a thermal conductivity detector.

2.3. Characterization in situ

X-ray photoelectron spectra (XPS) were obtained on a Perkin-Elmer Model No. 1257 Instrument using Al Kα as the radiation source, with energy of 1486.6 eV and 12 kV. The pass time was 0.2 s with scanning of 20, 100, 50, 30 and 10 for elements Zr (3d), Cl (2p), Al (2p), C (1s) and O (1s), respectively. For Pd (3d) 30 and 200 scanning were used in order to observe if photoreduction of Pd might occur after exposition to the X-ray beam. Correction of the charge effect was made with the C (1s) peak at 284.6 eV. Analyses were performed recording spectra of Pd (3d), Zr (3d), Cl (2p), Al (2p), C (1s) and O (1s), for the Pd/Al_2O_3 and Pd/ZrO_2 systems. Samples were pretreated with nitrogen and then methane oxidation was performed under stoichiometric reaction condition in a pre-chamber. After evacuation and cooling down,

Table 1
Chemical composition (w/w), surface area and dispersion of catalysts

Catalyst	Pd (wt.%)	S_{BET} (m^2/g)	CO chemisorption (μmolesCO/gcat)[a]	Dispersion (%)
Part a				
$Pd/Al_2O_3(Cl)$	0.96	200	26.7	29.4
Pd/ZrO_2	1.13	62	29.0	27.3

Catalyst	Pd (wt.%)	Nb_2O_5 (wt.%)	S_{BET} (m^2/g)	CO chemisorption (μmoles/mg_{Pd})[b]	Dispersion (%)
Part b					
PdAl(N)	0.84	–	162	2.13	19.2[b] (26.7)[a]
Pd10NbAl	0.98	8.72	179	1.73	18.1 (15.6)
PdNb	0.78	99.22	5	1.06	8.7 (7.3)

[a] After reduction at 500 °C.
[b] After reduction at 300 °C.

samples were introduced into the UHV chamber and spectra were obtained. In order to identify the oxidation states of palladium and zirconia during the oxidation of propane, the samples were submitted separately to 10% CH_4/He with 5% O_2/He, and 10% CH_4/He with 5% O_2/He, both under stoichiometric conditions ($R = 2.0$), at 20 mL/min and at 400 °C for 60 min. These experiments were performed ex situ in the pretreatment chamber and transferred into UHV chamber.

Diffuse reflectance infrared Fourier transform spectroscopy (DRIFTS) analyses have been carried in a Nicolet spectrometer (Nexus 470 model) with a MCT detector and equipped with a diffuse reflectance assembly (Spectra-Tech) chamber for high temperature treatment and ZnSe window. The experiment was carried out after in situ treatment with He (99.99%) at 400 °C for 1 h and 20 mL/min. Then, a mixture of $O_2 + CH_4$ (2:1) was flown at with 40 mL/min and the spectrum was taken after 6 h of reaction at 400 °C (similar to reaction conditions). All spectra were obtained after average of 64 scans and resolution of 4 cm^{-1}. The spectrum of the sample after He treatment was used as background. Two different procedures were used, first, with flowing gas mixture and in the closed chamber.

3. Results

3.1. Chemical composition and dispersion

Chemical compositions and textural data of two sets of catalysts are summarized in Table 1a and b.

Table 1a shows that although the surface area of Al_2O_3 is three times that of ZrO_2 support, the CO adsorption values are quite similar, with similar dispersions, around 29%, when reduced at 500 °C. That means, the catalysts reduced at 500 °C expose similar metallic Pd surface area, which is important for comparison.

On the other hand, the PdAl(N) and those modified with anchored Nb_2O_5 for a concentration of 10 wt.% in comparison with pure Pd/Nb_2O_5 catalysts, show that the specific surface area increased with 10% niobia content. The specific surface area of pure niobia is 5 m^2/g and much lower than alumina support. The metallic surface area was very similar to alumina support. The palladium content was also approximately 1% for all samples. The dispersion of Pd/Al_2O_3 of this set was quite similar to the previous one, however, the dispersion decreased with 10Nb content and was halved for Pd/Nb_2O_5 when compared to the Pd/Al_2O_3 catalyst, but lower than the Pd/ZrO_2 catalyst, which can be attributed to the different precursors and to the SMSI effect due to the migration of Nb_2O_5 over the Pd particles. Therefore, catalytic activities will be compared for the two sets of catalysts, as shown in sequence.

3.2. Methane oxidation

3.2.1. The Pd/Al_2O_3 and Pd/ZrO_2 systems

The overall reaction is:

$$CH_4 + 2O_2 \rightarrow CO_2 + 2H_2O, \quad \Delta H_{298\,K} = -802.7\,kJ/mol \tag{1}$$

This reaction is highly exothermic and the thermal effects are important in the combustion reaction. Fig. 1 shows that the ZrO_2 support is active for methane combustion above 620 °C, for an O_2/CH_4 ratio of 2 and reaches 25% of O_2 conversion at 800 °C, which must be taken in account after introduction of the metal.

3.2.1.1. Effect of pretreatment. The effect of the Pd state, oxide or metallic form, of Pd/Al_2O_3 and/$PdZrO_2$ catalysts on

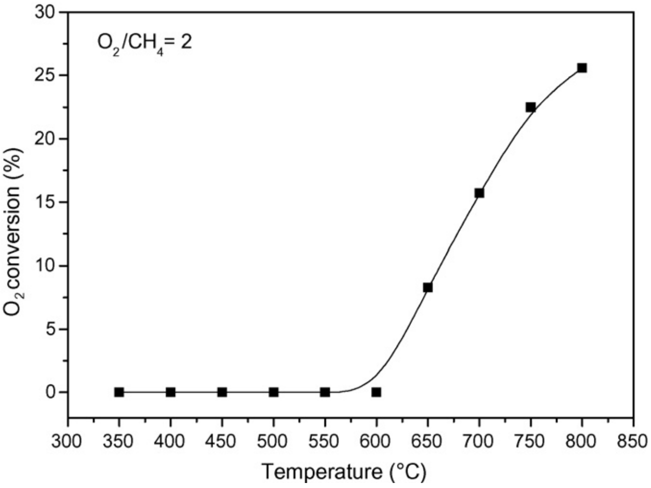

Fig. 1. Effect of the support—methane oxidation on ZrO_2.

methane oxidation is shown in Fig. 2A and B. The methane oxidation depends on the reaction temperature and shows that for the Pd/Al_2O_3 catalyst, starting with reduced palladium oxide, the conversion increases exponentially and is completed at 500 °C. However, starting with the PdO in the calcined form, the activity reaches a maximum at 450 °C and then decreases, probably due to the deactivation.

Unlikely is the behavior on the Pd/ZrO_2 catalyst, which displays significant differences. First, both calcined and reduced PdO display similar conversion below 350 °C and above 450 °C but the light off temperature of the reduced catalyst is 400 °C, while of the calcined catalyst is 450 °C, a difference of 50 °C. The deactivation starts at 500 °C. Curves show that the Pd/ZrO_2 catalyst is significant more active starting with the reduced PdO.

3.2.1.2. Induction time and stability. The stability of the catalysts for the methane combustion was tested for two temperatures at 350 and 400 °C; the light off temperatures of the Pd/ZrO_2 and Pd/Al_2O_3 catalysts are different, as shown previously for different pretreatment conditions. Results are shown in Fig. 3A and B. These results are quite important, firstly, because they show long induction times for both catalysts and secondly, although both deactivate with time on stream, the regeneration is different, which evidences different surface properties during the regeneration procedure. The induction times of the Pd/ZrO_2 and Pd/Al_2O_3 catalysts at 400 °C are around 3 and 4 h, respectively. However, the conversion on the Pd/Al_2O_3 catalysts goes instantaneously from 5 to 100% and deactivates abruptly to 10% after 15 h. After regeneration with oxygen, this catalyst was not regenerated at all. On the contrary, the Pd/ZrO_2 catalyst exhibits similar induction time after 3 h reaching 55% of conversion and deactivates similarly. After regeneration with oxygen it is partially recovered, attaining half of the initial activity, deactivating again after 5 h.

On the other hand, the stability test at 350 °C displays the conversion with time on stream for the Pd/ZrO_2 catalyst, and a marked stability after an induction period of 3–5 h and the activity goes instantaneously from 5 to 55% conversion. The Pd/Al_2O_3 catalyst did present a much smaller activity after an

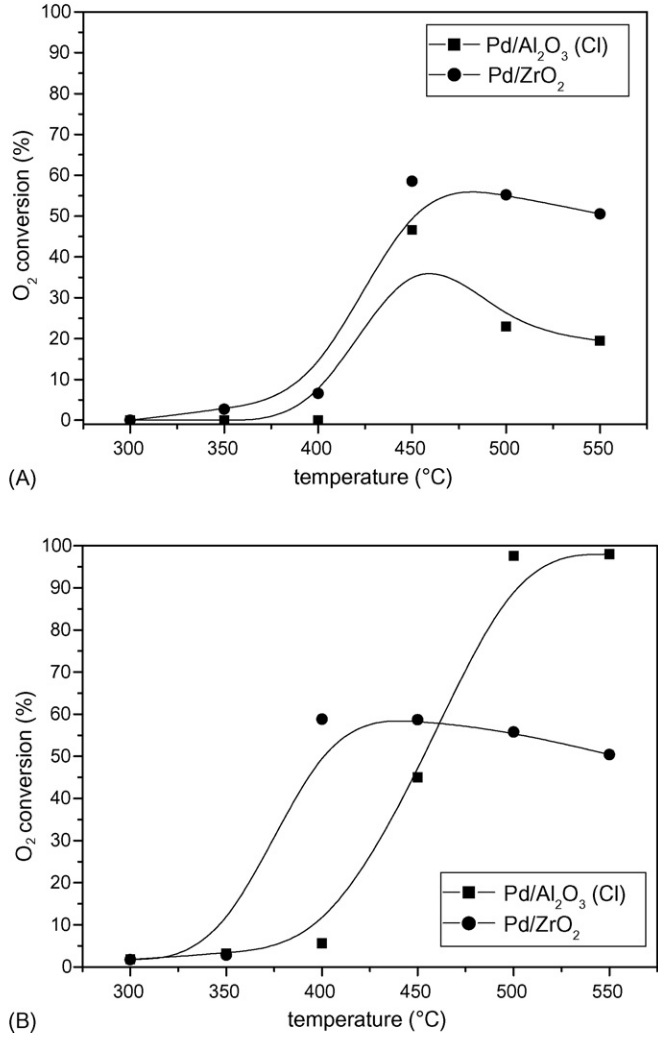

Fig. 2. Catalytic activities in terms of O_2 conversion as a function of temperature for total CH_4 oxidation with a feed composition of $O_2/CH_4 = 2$ and the following pretreatments: (A) without reduction and (B) with reduction at 500 °C for 1 h.

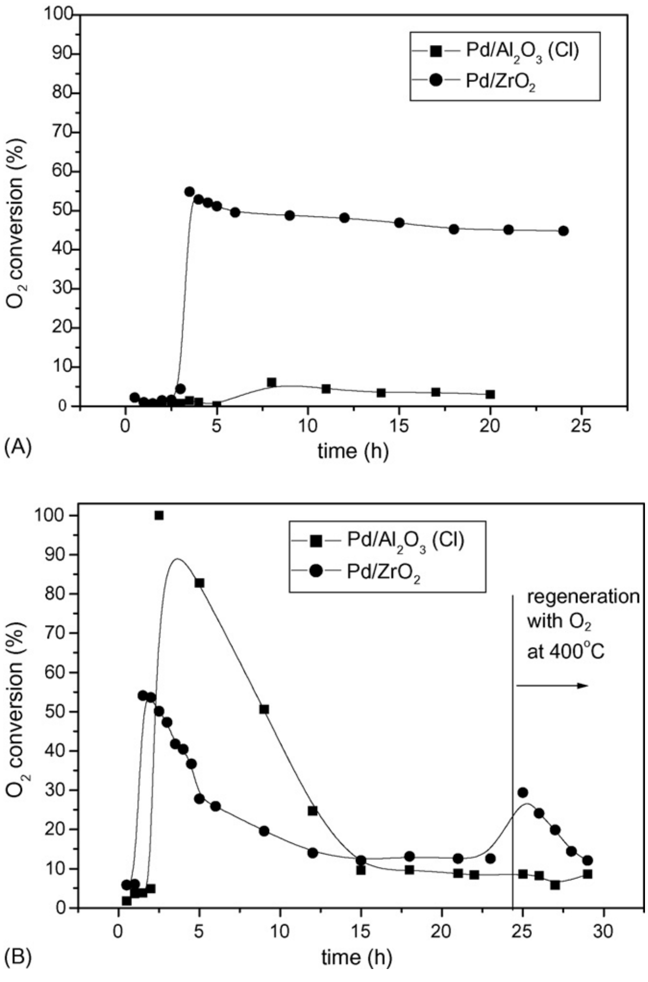

Fig. 3. Deactivation test in terms of O_2 conversion as a function of time on stream, with feed ratio of $O_2/CH_4 = 2$, at (A) 350 °C and (B) 400 °C. The catalysts were not pre-reduced.

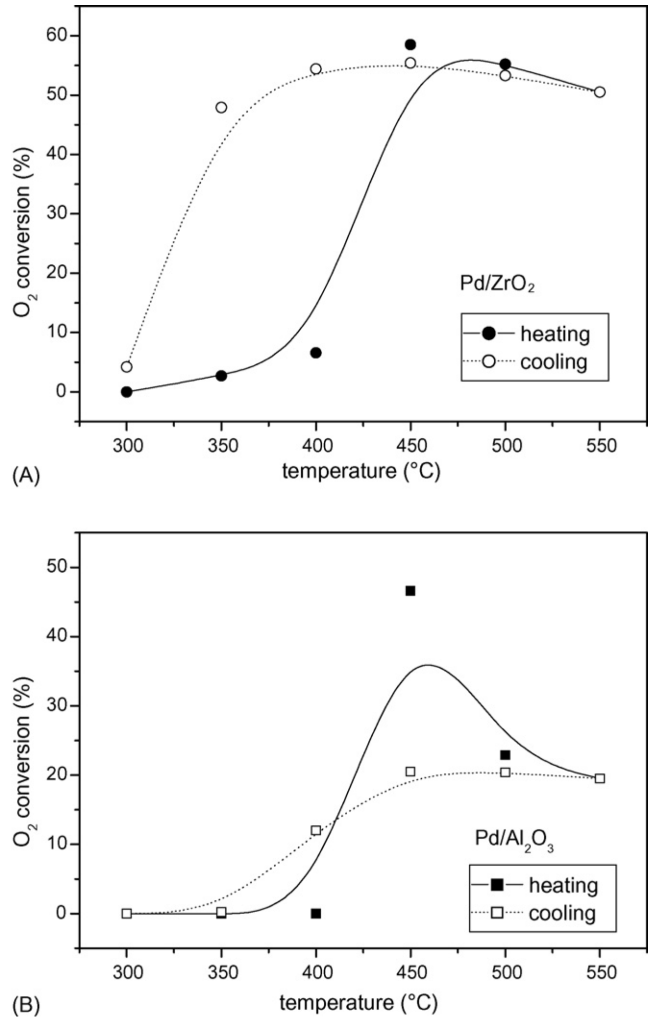

Fig. 4. Uprising and reversing temperature for Pd/ZrO$_2$ (A) and Pd/Al$_2$O$_3$ (B) catalysts. The catalysts were not reduced.

induction time of 5 h. The deactivation process under these conditions is apparently much slower than at 400 °C.

3.2.1.3. Downwards temperature effect. This effect has been mentioned in the literature and Fig. 4 displays the conversion of oxygen in the methane combustion uprising the temperature and after reaching the maximum conversion the temperature was lowered following the conversion, indicating a downwards procedure.

The conversion increases with rising the temperature, showing a light off temperature of 450 °C and instantaneously increases up to 100% conversion for Pd/ZrO$_2$ catalyst. Downwards the conversion remains stable at 100% until 350 °C and decreases to the initial starting temperature conversion, indicating that the PdO surface was markedly modified during the uprising temperature, remaining then stable and very active. The Pd/Al$_2$O$_3$ catalyst exhibited lower stability than the Pd/ZrO$_2$ during downwards procedure.

3.2.2. The Pd/Nb$_2$O$_5$ and Pd/Nb$_2$O$_5$/Al$_2$O$_3$ systems

The temperatures required for conversion of 10% ($T_{10\%}$) of methane for the catalysts are summarized in Table 2.

Table 2
Temperatures required for reaching 10% of methane conversion

Catalyst	$T_{10\%}$ (°C) O$_2$/CH$_4$ = 2	$T_{10\%}$ (°C) O$_2$/CH$_4$ = 4
PdAl	321	323
Pd10NbAl	405	400
PdNb	493	520

The ignition temperature (T_{10}) over Pd/Al$_2$O$_3$ was 321 °C and the conversion increases sharply with temperature up to 500 °C, reaching 90% conversion. This behavior is in accordance with published data concerning similar Pd/Al$_2$O$_3$ systems [15–17].

Ignition temperature can be conveniently taken as a measure of activity, allowing us to set the sequence PdAl > Pd10N-Pd10NbAl > ≈PdNb. The results showed that the presence of niobia affects negatively the catalyst performance as the ignition temperature raises 84 °C for Pd10NbAl sample when compared to bare PdAl catalyst. There are no significant differences for stoichiometric condition and with excess of oxygen.

Fig. 5 presents the conversion of CH$_4$ with the temperature for different catalysts for methane combustion with oxygen in excess. Carbon dioxide and water were the only reaction products detected during the experiments. The results indicated that the required reaction temperature for methane isoconversion increased more on the PdNb than on the Pd10NbAl catalysts. The methane conversion starts at about 300 °C for PdAl. This is the most active catalyst, in agreement with other reported data in the literature. The Pd10NbAl catalyst exhibits lower activity and a higher temperature, being the PdNb catalyst the less active.

From Fig. 5 it is possible to evaluate the reaction temperature or the activity at isoconversion (conversion of methane or oxygen) around 13–15%, as presented in Table 3.

3.3. Characterizations in situ

Stability tests are presented in Fig. 5. Worth notice is the induction time for the Pd/Al$_2$O$_3$ and Pd/ZrO$_2$ catalysts. They present different stabilities and activities. After 3 h with TOS the oxygen conversion suddenly increases by a factor of 10 and progressively stabilizes after 10 h, and depending of the reaction temperature the catalyst is deactivated.

XPS measurements were carried out on Pd/Al$_2$O$_3$ and Pd/ZrO$_2$ catalysts at constant temperature of 400 °C for long periods until 10 h and analyzed after different reaction times in situ. XPS results obtained after treatment in a pre-chamber submitted to similar conditions (T = 400 °C, O$_2$/CH$_4$ = 2) and then analyzed under vacuum at 10^{-10} Torr, showed Pd 3d$_{3/2}$ and Pd d$_{5/2}$ peaks after different times, displayed in Fig. 6A and B. Fig. 6A displays the lineshapes of Pd/Al$_2$O$_3$ after 2 and 10 h, which are very similar, indicating only PdO species at the surface.

Fig. 6B shows the XPS results on Pd/ZrO$_2$ displaying a visible satellite peak at 337.6 eV after 10 h, suggesting the presence of PdO$_x$ species formation only after 10 h reaction

Table 3
Temperature at isoconversion for different supports and precursors

Conversion of CH_4 or O_2 (%)	Pd/Al_2O_3(Cl)	Pd/ZrO_2(Cl)	Pd/Al_2O_3(N)	$Pd/Nb_2O_5/Al_2O_3$(N)	Pd/Nb_2O_5(N)
13–15	≈420	≈415	325	420	530

exposition, indicating modification of PdO at the surface. These results suggest strongly that the oxidation state of PdO at the surface modifies during the reaction on both supports. Fig. 6B shows also the Zr $3p_{1/2}$ and Zr $3p_{5/2}$ peaks without modification compared to the calcined sample.

Table 4a presents the binding energy values of Pd $3d_{5/2}$ and Pd $3d_{3/2}$ and the Pd/Al atomic ratios at the surface with time on stream. Notice that the bond energy up to 6 h is 336.9 eV, which corresponds to the PdO species at the surface. After 10 h the bonding is shifted to 337.1 eV. In addition, the peak area of Pd 3d is initially high and decreases 9-fold after 2 h, recovering partially half of the initial area after 10 h. Indeed, the Pd/Al atomic ratios decreased with increasing time of reaction exposition and are half of the initial PdO particles at the surface after 10 h reaction, which suggests agglomeration of the initial PdO particles. Noteworthy is that no metallic Pd was detected at the surface at all during various reaction times, which is not in accordance with the reported references concerning the redox phenomena at the surface on the Pd/Al_2O_3 catalyst.

Table 4b presents the binding energy Pd/ZrO_2 catalyst after 10 h with time on stream. The binding energies up to 6 h with time on stream (not shown) were absolutely similar to the binding energies of Pd/Al_2O_3 catalyst. However, suddenly after 10 h reaction the binding energy for Pd $3d_{5/2}$ increased towards 337.6 eV, and according to the literature corresponds to a higher oxidation state of PdO_x or $PdO^{\delta+}$. The Pd/Zr surface atomic ratio is 2.7×10^{-2} and when compared to the Pd/Al_2O_3 catalyst increased 10 times, indicating a pronounced augment of palladium at the surface with a higher oxidation state of $Pd^{2+\delta}$.

The induction time of our results is approximately 3–5 h, which corroborates with the hypothesis of rearrangement of the PdO in a higher oxidation state and stabilization of this

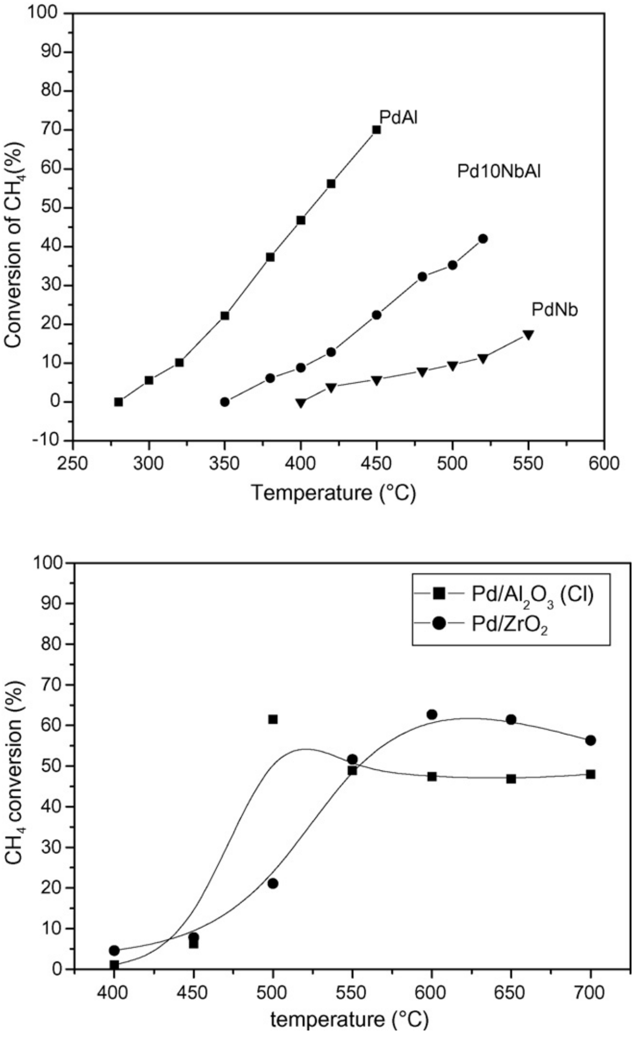

Fig. 5. Conversion of methane to CO_2 as function of the temperature for total oxidation of methane (CH_4:O_2 = 1:4) for different catalysts.

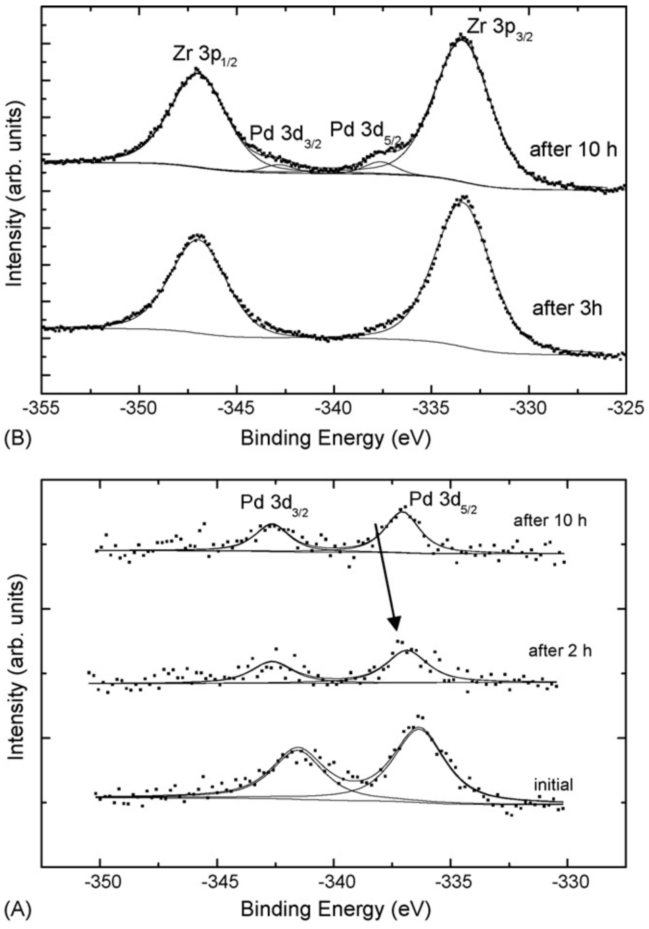

Fig. 6. XPS in situ reaction on Pd/Al_2O_3 (A) and Pd/ZrO_2 (B) catalyst.

Table 4a
Electron binding energies and atomic ratios for Pd/Al_2O_3 catalyst

Time (h)	Energy (eV)		Area		Pd/Al
	Pd $3d_{5/2}$	Pd $3d_{3/2}$	Al 2p	Pd 3d	
0	336.3	341.6	1907	243.2	5.6×10^{-3}
2	336.9	342.6	1663	35.3	9.3×10^{-4}
6	336.9	342.6	1448	71.0	2.1×10^{-3}
10	337.1	342.6	1796	95.4	2.3×10^{-3}

Table 4b
Electron binding energies and atomic ratios for Pd/ZrO_2 catalyst

Time (h)	Energy (eV)		Area		Pd/Zr
	Pd $3d_{5/2}$	Pd $3d_{3/2}$	Zr 3d	Pd 3d	
10	337.6	342.8	9642	534	2.7×10^{-2}

oxidation state at the surface. The downwards procedure experiments on both catalysts evidence that once the PdO/PdO_x is stabilized the activity is still high reducing the methane oxidation temperature by 100 °C. On the other hand, stability tests showed that the Pd/ZrO_2 catalyst was more stable than the Pd/Al_2O_3 catalyst, in particular for 350 °C. On the contrary, the Pd/Al_2O_3 catalyst deactivated and is not regenerated. It turns out, that in the Pd/ZrO_2 the ZrO_2 is capable to storage oxygen supplied by molecular oxygen at the surface, due to the interaction of PdO_x/ZrO_y interface.

It is well known that some carriers, such as CeO_2 and TiO_2, provide structural oxygen to the Pd metal during reoxidation, which is then replenished from the gas phase. Each of these supports has labile oxygen and can change the valence state. Farrauto et al. [6] showed that independent of the support the PdO-Pd transformation occurs during the reduction/decomposition. The TGA experiments were similar, reducing the Pd/Al_2O_3 sample up to 500 °C and subsequently passing He flow and cooling to 400 °C. Then switching to a O_2/He mixture and raising the temperature up to 900 °C and cooling again to 400 °C as indicated in Fig. 7. The cycle was repeated twice. Results indicate that after reduction the metallic Pd is oxidized to PdO during cooling in oxygen flow around 580 °C where a little gain of 0.06% is observed, which is not sufficient to oxidize Pd^0 in PdO, suggesting a little change in the oxidation state of PdO. XPS results did show only PdO and $PdO^{\delta+}$ in a higher oxidation state. It suggests that here there is surface modification of PdO/$PdO^{\delta+}$ state during the methane oxidation experiments, which may be the active sites at the surface.

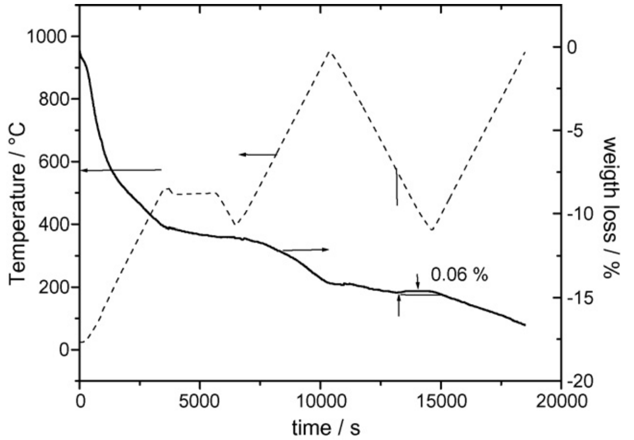

Fig. 7. TGA measurements on Pd/Al_2O_3 with different procedures: reduction, oxidation, heating and cooling with different temperature cycles.

The ‘‘in situ’’ DRIFTS results of methane oxidation reaction on Pd/Al_2O_3 and Pd/ZrO_2 catalysts are presented in Fig. 8A and B. Two different sets were obtained with flow and closed chamber. The presence of the different products was determined identifying the adsorption bands, according to the literature.

Fig. 8 displays the bands in the region of 2500–100 cm^{-1} (Fig. 8A) and 3200–2500 cm^{-1} (Fig. 8B), both figures show the spectra taken in flow of reaction (a and c) and with closed chamber (b and d) to Pd/Al_2O_3 (a and b) and Pd/ZrO_2 (c and d)

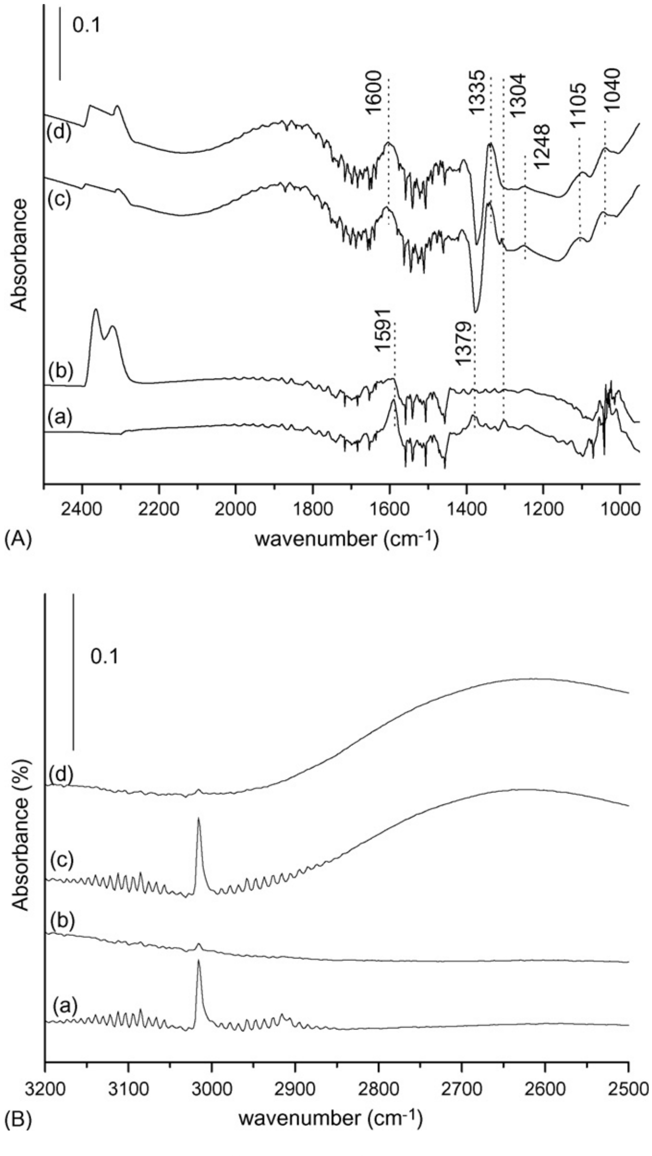

Fig. 8. DRIFT spectra at different regions for Pd/Al_2O_3 (c and d) and Pd/ZrO_2 (a and b). The analyses were made under flow (a and c) and in closed chamber (b and d).

catalysts. The Pd/Al_2O_3 exhibits bands at 1591, 1379, 1304 cm^{-1} (Fig. 8A) and 3016, 2909 cm^{-1} (Fig. 8B). The bands raised at 1591 (ν_{as} C–O), 1379 (δ_s C–H), and 2909 cm^{-1} (ν C–H) can be attributed to formate species [18]; while bands at 3016 cm^{-1} (ν C–H) and 1304 cm^{-1} (δ C–H) are due to CH_4 gas. Low intensity bands are present in the range of 1100–1000 cm^{-1} and could indicate carbonate (ν C–O) species formation, however it is difficult to ascertain it precisely once the other characteristic vibration modes are in the same region of formate species. According to the literature [19], monodentade carbonate exhibits bands at 1530–1470 cm^{-1} (ν_{as} COO^-), 1300–1370 cm^{-1} (ν_s COO^-), 1080–1040 (ν C–O); and bidentade 1530–1620 cm^{-1} (ν C–O), 1270–1250 cm^{-1} (ν_{as} COO), 1030–1020 (ν_s COO) or 1620–1670 cm^{-1} (ν C–O), 1220–1270 cm^{-1} (ν_{as} COO), 980–1020 (ν_s COO) depending on the adsorption mode. In the closed system, methane and formate are released and CO_2 gaseous species are observed at 2350 cm^{-1} suggesting decomposition of formate into CO_2.

Concerning to Pd/ZrO_2 catalyst, important differences were observed (Fig. 8c and d). Notice that no formate species are present and the bands at 1600, 1335, 1248 and 1040 cm^{-1} can be attributed to carbonates [13,19], which are strongly adsorbed once the experiment with closed chamber a slight decrease in these bands was observed and lower CO_2 formation. Li et al. [13], in the methane oxidation study over Pd/Al_2O_3 and Pd/Co_3O_4 catalysts using infrared analyses, indicated that O_2^- species are formed in the region of 1200–1050 cm^{-1}. In our system, the lower intensity band at 1105 cm^{-1} could be tentatively attributed to O_2^- adsorbed at Pd/ZrO_2 catalyst.

4. Discussion

4.1. Catalytic tests

The calcined Pd/ZrO_2 presented higher activity and stability than the Pd/Al_2O_3, according to Fig. 2. The Pd/ZrO_2 catalyst showed similar behavior after calcination and reduction pretreatments, with a minor shift of activation toward lower temperature after pre-reduction. On the other hand, pretreatment affected greatly the activity of Pd/Al_2O_3 at high reaction temperatures (>500 °C). Although the pre-reduced Pd/Al_2O_3 exhibits higher activity above 500 °C, it is an unstable phenomenon, as seen in the stability tests. Müller et al. [20] observed that the reduced Pd/ZrO_2 catalyst presented higher activity than the unreduced catalyst. Su et al. [21] showed that the reduction of PdO by methane occurs via a nucleation mechanism and requires the presence of metallic Pd. They claim that the presence of small amounts of Pd^0 decreases the light-off temperature of Pd/ZrO_2 catalyst.

The catalytic tests performed with excess of O_2 in the feedstream ($O_2/CH_4 = 4$), Fig. 5B, showed that the activation of Pd/ZrO_2 was slower than that of Pd/Al_2O_3, but more stable. A comparison between Figs. 2A and 5B clearly shows that the excess of O_2 decreases the catalytic activities. According to the mechanism proposed by Fujimoto et al. [11], the rate-limiting step for methane oxidation is the dissociative sorption of CH_4 on a site pair consisting of adjacent Pd surface vacancies and surface Pd-O species. Consequently, the catalytic activity in the methane oxidation of supported palladium catalysts depends on the oxidation state of palladium, which depends of the catalyst pretreatment and the O_2/CH_4 ratio of the reaction mixture. With increasing O_2/CH_4 ratio, the oxidation of metallic palladium proceeds extensively, leading to a less active phase, and therefore, the activity of the catalyst decreases, in agreement with Yang et al. [22].

In relation to the stability tests presented in Fig. 3, at 350 °C, Pd/Al_2O_3 did not present any activation, while Pd/ZrO_2 is activated after 3 h on stream, with stable activity up to 25 h. At 400 °C, Pd/Al_2O_3 reached total O_2 conversion after 2 h on stream but exhibits fast deactivation. It was not regenerated after pretreating with O_2 at 400 °C. The Pd/ZrO_2 presented also a continuous deactivation with time on stream at 400 °C but it was partially regenerated after O_2 treatment. The O_2 may be changing the equilibrium $PdO \leftrightarrow PdO_x$, restoring the active phase of the catalyst, and/or promoting the oxidation of the coke deposits formed by methane decomposition. The higher stability of Pd/ZrO_2 was also demonstrated in the test with excess of O_2.

Eppling and Hoflund [12] also studied the influence of the support over the activity and stability of palladium catalysts, showing that Pd/ZrO_2 exhibits better performance than Pd/Al_2O_3 at 250 °C, maintaining its activity for over 130 h on stream. The initial activation period during methane combustion can be related to the presence of oxygen-deficient PdO_x crystallites, which contain stronger Pd-O oxygen bonds and increase their oxygen content during reaction [11], or it can be associated with the removal of residual chloride from catalyst surface, which strongly inhibits the conversion of methane [23]. Under reaction conditions, chlorine ions originating from the precursor ($PdCl_2$) are removed by water formation during combustion, producing HCl. According to Yang et al. [22], the higher activity of Pd/ZrO_2 in relation to Pd/Al_2O_3 can be related to oxygen mobility, which is about three times higher on zirconia than on alumina. According to the literature, the redox mechanism for methane combustion involves the mobility of oxygen: gaseous oxygen first adsorbs strongly onto metallic particles forming a surface palladium oxide; methane then adsorbs on this oxidic surface and is oxidized to CO_2 and H_2O, while at the same time the palladium oxide is reduced to the metallic state [5]. However, Li et al. [13] reported recently a different interpretation mechanism, based on DRIFTS experiments, that are in contradiction with previous results [5,6,12]. Our experiments did show similar behavior but different parameters are needed to explain the induction time, activity and reverse stability, which can be observed from the in situ experiments.

4.1.1. Effect of support and precursor

The set of experiments with Pd/Al_2O_3 and Pd/ZrO_2 catalysts was prepared using chloride ($PdCl_2$), while the set of Pd/Al_2O_3, Pd/Nb_2O_5 and $Pd/10Nb_2O_5/Al_2O_3$ the nitrate ($Pd(NO_3)_2$) precursors. Dispersions for the Pd/Al_2O_3 catalysts indicated similar values for each set and different precursors. With chloride precursor the dispersions for Pd/ZrO_2 catalysts were of the order of 28%, after reduction at 300 and 500 °C, while with nitrate the dispersions were of the order of 19–26%, after reduction at 300 and 500 °C, respectively, suggesting similar particle sizes. It means that particle size effects are comparable for each set.

The Pd/Nb_2O_5 and Pd/10Nb_2O_5/Al_2O_3 presented, after reduction at 300 and 500 °C, lower dispersions than the Pd/Al_2O_3 catalyst (Table 1b), suggesting some SMSI effect. Since during the oxidation of methane there is water formation, that should destroy the SMSI effect, and therefore the activity is not altered.

For niobia-based catalysts, the methane oxidation rate decreases with the niobium oxide sublayer. According to the literature, methane oxidation is favored on larger Pd particles. It seems that NbO_x species are formed during the reaction, preventing the surface exposition of PdO active sites. Depending on the Nb loading the activity changed, indicating a modification in the surface phenomena PdO and $PdO^{\delta+}$ during the reaction, associated with the weak bonding of PdO–NbO_x at the surface.

Thevenin et al. [14] studied methane conversion over Pd/Al_2O_3, Pd/La-Al_2O_3 and Pd/Ba-Al_2O_3 samples and did not observe major differences with respect to the catalytic activity of Pd-supported catalysts for total oxidation of methane. All catalysts presented a similar ignition path, about 470 °C ($T_{10\%}$, temperature for 10% conversion), regardless of the nature of the support material and apparent reaction rate. Wang et al. [9] studied the effects of titania on the Pd/Al_2O_3 for methane combustion, contrary to our results. Their results indicate a positive effect on the activity with increasing TiO_2 loading of Pd/x%TiO_2–Al_2O_3 catalysts. The temperature required for 10% ($T_{10\%}$) conversion of methane was 350 °C for the 1.10%Pd/TiO_2 catalyst. These catalysts cannot resist temperatures higher than 650 °C. It was attributed to the migration of TiO_2 onto palladium crystallites. Fraga et al. [15] verified that addition of tin and lanthanum on PdO/Al_2O_3 did not bring any benefit to the activity in methane combustion.

Lee and Trimm [24] have reported that the kinetics of catalytic combustion is only relevant at low conversions. Once the light-off occurs, mass and heat transfer are the important parameters. Therefore, the porosity of the catalyst/support have much more effect in the higher region of conversion and the reaction rapidly approaches complete conversion and the heat generated from combustion results in a significant increase in the catalyst temperature.

It turns out that the precursor may influence the activity inducing that the nitrate precursor favors the formation of larger particles of PdO at the surface of the support and thus according to the literature affects positively the methane oxidation. The activities of Pd/Al_2O_3(Cl), Pd/ZrO_2(Cl) and Pd/Nb_2O_5/Al_2O_3(N) are approximately similar when compared at low isoconversion. The Pd/Nb_2O_5 catalyst is less active, more than 100 °C is needed to get the same conversion. Farrauto et al. [6] reported that the catalytic activity for methane conversion is strongly dependent on the nature of the support, in particular comparing Al_2O_3 with ZrO_2, CeO_2, TiO_2 with metal as active phase, promoting or inhibiting the reoxidation at different temperatures, depending of the labile oxygen or not. These results show that the activity is dependent of the dispersion of Pd and the interaction of PdO with the support surface, which depends on the precursor. It depends particularly on the capacity of oxygen transfer from the support to the palladium oxidation state. For Pd/Al_2O_3 the effect of precursor is important, however for the Pd/ZrO_2, Pd/Nb_2O_5/Al_2O_3 and Pd/Nb_2O_5 the palladium oxidation state should be affected, influencing the activity on methane oxidation.

4.2. Reaction mechanism

It seems that there are two different reaction mechanisms. XPS results confirm the presence of PdO in the higher oxidation state and not metallic Pd. This excludes the redox phenomenon PdO ↔ Pd^0, as reported in the literature. XPS results suggest the formation of Pd oxides of different oxidation states. $PdO^{\delta+}$ is formed during the induction period, which coexists with PdO at the surface, in accordance with TGA results, and may be responsible for the activity and stability of the catalysts. On the other hand, DRIFTS results showed formate at the surface of the Pd/Al_2O_3 catalyst, confirming the proposed model of Li et al. [13], where formate and $PdO^{\delta+}$ are formed during the methane oxidation.

On the other hand, DRIFTS results did not show formate on the Pd/ZrO_2 catalyst but CH fragment species (1335 cm^{-1}) and particularly O_2^- adsorption bands (1105 and 1040 cm^{-1}). The reaction mechanism suggests that the adsorption of O_2^- occurs at the ZrO_x surface, which reacts with gas CH_4 and forms CH_3^- radicals. These radicals favor the formation of carbonate or bicarbonate species, which decomposes in CO_2. PdO and $PdO^{\delta+}$ are the surface active phases, and the interaction with $PdO^{\delta+}$ provoke the reduction of surface $ZrO^{\delta-}$, attracting the O_2 in the gas phase to adsorbed as O_2^-.

The reaction scheme for the Pd/Al_2O_3 is in accordance with the proposed mechanism by Li et al. [13]. However, for the Pd/ZrO_2 catalyst the following reactions are suggested based on XPS, TGA and DRIFTS:

$$Pd^{2+} \rightarrow Pd^{4+} + 2e^-$$

$$O_2(g) + 2e^- \rightarrow 2{O_s}^{2-}$$

$$Pd^{4+} + {O_s}^{2-} \rightarrow Pd{-}{O_s}^{2-}$$

$$Zr^{4+} + {O_s}^{2-} + CH_4 \rightarrow Zr^{n+} + {CH_3}^- + {HCO_3}^- + e^-$$

$$Pd^{4+}{-}{CH_3}^- + Zr^{4+} \Leftrightarrow Pd^{4+} + Zr^{4+}{-}CH_{3ads}$$

$$Pd{-}{O_s}^{2-} + Zr^{4+} \Leftrightarrow Pd^{4+} + Zr^{4+}{-}{O_s}^{2-}$$

$$Pd^{4+} + 2e^- \rightarrow Pd^{2+} + {O_2}^-{}_{ads}$$

$$Zr^{n+} \rightarrow Zr^{4+} + e^-$$

$$HCO_3^- \rightarrow CO_2(g) + H_2O$$

5. Conclusions

The methane oxidation is dependent of the precursor affecting the dispersion. Nitrate precursor diminishes the dispersion, affecting particle sizes, and hence increases the activity.

The Pd/ZrO_2 catalyst is initially not more active than Pd/Al_2O_3, but provides sufficient oxygen during the induction time to enhance the oxidation state of PdO and the stability of PdO in different oxidation states, according to XPS and TGA results, allowing to a higher stability and activity with less deactivation. The coexistence of PdO/$PdO^{\delta+}$ interface allows the activation of the surface, independent of the support.

DRIFTS results showed that after surface activation the Pd/Al_2O_3 allows the formation of a formate species at the interface PdO/$PdO^{\delta+}$, with the formation of carbonate species. On the other hand, the Pd/ZrO_2 catalyst did not form formate but CH fragments and adsorption of oxygen $O_2{}^-$ at the surface of ZrO_2, due to the reduction of ZrO^{n+} at the interface of PdO/$PdO^{\delta+}$, and thus a different reaction mechanism.

References

[1] T.R. Baldwin, R. Burch, Appl. Catal. 66 (1990) 337.
[2] F.H. Ribeiro, M. Chow, B.R.A. Dalla, J. Catal. 146 (1994) 537.
[3] R. Burch, F.J. Urbano, Appl. Catal. A: Gen. 124 (1995) 121.
[4] C.F. Cullis, T.G. Nevell, D.L.J. Trimm, Chem. Soc. Faraday Trans. 68 (1972) 1406.
[5] E. Garbowski, C. Feumi-Jantou, N. Mouaddib, M. Primet, Appl. Catal. A: Gen. 109 (1994) 277.
[6] R.J. Farrauto, J.K. Lampert, M.C. Hobson, E.M. Waterman, Appl. Catal. B: Environ. 6 (1995) 263.
[7] M. Lyubovsky, L. Pfefferle, Appl. Catal. A: Gen. 173 (1998) 107.
[8] T.J. Toops, A.B. Walters, M.A. Vannice, Appl. Catal. A Gen. 233 (2002) 125.
[9] C.B. Wang, H.G. Lee, T.F. Yeh, S.N. Hsu, K.S. Chu, Thermochim. Acta 71203 (2002) 1.
[10] F.B. Noronha, D.A.G. Aranda, A.P. Ordine, M. Schmal, Catal. Today 57 (2000) 275.
[11] K. Fujimoto, F.H. Ribeiro, M. Avalos-Borja, E. Iglesia, J. Catal. 179 (1998) 431.
[12] W.S. Eppling, G.B. Hoflund, J. Catal. 182 (1999) 5.
[13] Z. Li, G. Xu, G.B. Hoflund, Fuel Proc. Tech. 84 (2003) 1.
[14] P.O. Thevenin, A. Alcade, L. Petterssoon, S.G. Järas, J.L. Fierro, J. Catal. 215 (2003) 78.
[15] M.A. Fraga, E. Soares de Souza, F. Villain, L.G. Appel, Appl. Catal. A: Gen. 259 (2004) 57.
[16] K. Sckizawa, H. Widjaja, S. Maeda, Y. Ozawa, K. Eguchi, Appl. Catal. A: Gen. 200 (2000) 211.
[17] K. Eguchi, H. Arai, Appl. Catal. A: Gen. 222 (2001) 359.
[18] L.H. Little, Infrared Spectroscopy of Adsorbed Species, Academic Press, NY, 1966.
[19] A.A. Davydov, Infrared Spestroscopy of Adsorbed Species on the Surface of Transition Metal Oxides, John Wiley & Sons, NY, 1990.
[20] C.A. Müller, M. Maciejewski, R.A. Koeppel, A. Baiker, Catal. Today 47 (1999) 245.
[21] S.C. Su, J.N. Carstens, A.T. Bell, J. Catal. 176 (1998) 125.
[22] S. Yang, A. Maroto-Valente, M. Benito-Gonzalez, I. Rodriguez-Ramos, A. Guerrero-Ruiz, Appl. Catal. B 28 (2000) 223.
[23] D. Roth, P. Gélin, M. Primet, E. Tena, Appl. Catal. A 203 (2000) 37.
[24] J.H. Lee, D.L. Trimm, Fuel Proc. Tech. 42 (1995) 339.